PERGAMON

Available online at www.sciencedirect.com
SCIENCE DIRECT®

Polyhedron 22 (2003) 2573–2580

POLYHEDRON

www.elsevier.com/locate/poly

The reactivity of *mer*-[$ReOBr_3$(bipy)] towards gaseous nitric oxide. The crystal, molecular and electronic structure of *mer*-[$ReOBr_3$(bipy)] and [$ReBr_4$(bipy)]

Barbara Machura[a,*], J.O. Dzięgielewski[a], R. Kruszynski[b], T.J. Bartczak[b], J. Kusz[c]

[a] *Department of Inorganic and Radiation Chemistry, Institute of Chemistry, University of Silesia, 9th Szkolna Street, 40-006 Katowice, Poland*
[b] *X-ray Crystallography and Crystal Chemistry Laboratory, Institute of General and Ecological Chemistry, Technical University of Łódź, 116 Żeromski Street, 90-924 Lodz, Poland*
[c] *Institute of Physics, University of Silesia, 4th Uniwersytecka Street, 40-006 Katowice, Poland*

Received 16 January 2003; accepted 1 April 2003

Abstract

The reactivity of *mer*-[$ReOBr_3$(bipy)] (**1**) (bipy = bipyridine) towards gaseous nitric oxide has been investigated. The reaction of **1** with NO in bromoform has afforded only starting material, but in the presence of an excess of triphenylphosphine, the [$ReBr_3$(NO)(bipy)] (**3**) has been obtained. Refluxing of **1** and PPh_3 in $CHBr_3$ has led to the isolation of [$ReBr_4$(bipy)] (**2**). The complexes **1**, **2** and **3** were characterised by IR, UV–Vis and magnetical measurements. Crystal and molecular structures of **1** and **2** have been determined.

Keywords: Rhenium; Nitrosyl; Oxo; Bipyridine; X-ray structures; Electronic structures

1. Introduction

Nitrosyl transition metal complexes, their synthesis methods, the bonding nature of NO to metal centres, catalytic activities, capacity for pollution control and electron-transfer properties have attracted considerable interest for many years [1–7].

The discovery of the key role of nitric oxide in human cardiovascular and nervous systems, and in immune response to pathogen invasion, has resulted in an increase in the interest of nitrosyl transition metal complexes. These compounds are considered as potential deliverers of NO to biological targets upon demand either by thermal reactions or by photochemical excitation [8–10].

In our previous papers, we reported on the structural and spectroscopic characterisation of the nitrosyl rhenium complexes obtained in the reactions between the [$ReOX_3L_2$] complexes ($X = Cl$, Br, $L = PPh_3$ and $AsPh_3$) and gaseous nitric oxide [11–21].

Considering that rhenium nitrosyl complexes with chelating or bridging bidentate ligands in the coordination sphere are very rare [22–24], we are extending our studies to the reactivity of *mer*-[$ReOBr_3$(bipy)] (**1**) towards NO.

Here, we present spectroscopic and structural characterisation of the starting oxocomplex **1**, the chemistry of which is relatively unexplored [25,26], spectroscopic properties and crystal determination of [$ReBr_4$(bipy)] (**2**) obtained in the reaction between **1** and PPh_3 in refluxing $CHBr_3$, and spectroscopic characterization of [$ReBr_3$(NO)(bipy)] (**3**) isolated in the reaction of **1** with NO in the presence of PPh_3.

---

* Corresponding author. Tel.: +48-32-258-2441; fax: +48-32-259-9978.

E-mail addresses: basia@tc3.ich.us.edu.pl (B. Machura), tadekbar@ck-sg.p.lodz.pl (T.J. Bartczak).

0277-5387/03/$ - see front matter
doi:10.1016/S0277-5387(03)00350-4

2. Experimental

2.1. General considerations

Triphenylphosphine, 2,2′-bipyridine and ammonium perrhenate were purchased from Aldrich Chemical Co. and used without further purification. Solvents were obtained from commercial sources and thoroughly deoxygenated prior to use. The reactions were carried out under argon atmosphere.

Gaseous NO, obtained in the reaction:

$$2NaNO_2 + 3H_2SO_4 + 2FeSO_4 \rightarrow 2NO + 2NaHSO_4 + Fe_2(SO_4)_3 + 2H_2O$$

was purified by passing through washers with concentrated KOH solution and over solid NaOH.

Infrared spectra were recorded on a Nicolet Magna 560 spectrophotometer in the spectral range 4000–400 cm^{-1} with the samples in the form of potassium bromide pellets. Electronic spectra were measured on a spectrophotometer Lab Alliance UV–Vis 8500 in the range 800–220 nm in deoxygenated dichloromethane solution. Magnetic susceptibilities were measured at 296 K by the Faraday method.

2.2. Preparation of [ReOBr$_3$(bipy)] (1)

mer-[ReOBr$_3$(bipy)] was prepared according to the literature [25].

IR (KBr, cm^{-1}) 3111 (m), 3080 (m), 1605 (s), 1495 (w), 1475 (s), 1442 (s), 1321 (s), 1236 (w), 1174 (w), 1232 (w), 1173 (w), 1124 (w), 1071 (w), 1030 (w), 982 (s), 771 (s), 747(w) 725 (m), 664 (w), 650 (w), 429 (w).

Anal. Found: C, 20.20; H, 1.40; N, 4.60. Calc. for $C_{10}H_8N_2Br_3ORe$ (**1**): C, 20.08; H, 1.35; N, 4.68%.

2.3. Preparation of [ReBr$_4$(bipy)] (2)

The *mer*-[ReOBr$_3$(bipy)] complex (0.5 g, 0.84 mmol) was added to a solution of PPh$_3$ (1 g, 3.8 mmol) in bromoform (60 cm^3) and was refluxed for 4 h. The colour changed quickly from green to dark red. The volume was condensed to 10 cm^3 and a reddish-brown microcrystalline solid was formed by the addition of 100 cm^3 of EtOH. The product was washed with EtOH and cold ether, and dried in vacuo.

The crystals of **2** suitable for X-ray investigation were obtained by recrystallization from CHCl$_3$–EtOH. (Yield: 60%). IR (KBr, cm^{-1}) 3110 (m), 3078 (m), 1601 (s), 1565 (w), 1494 (m), 1467 (s), 1446 (s), 1417 (w), 1315 (m), 1235 (w), 1173 (w), 1235 (w), 1173 (w), 1122 (w), 1105 (m), 1069 (m), 1032 (m), 1020 (m), 768 (s), 722 (m), 664 (w), 650 (m).

Anal. Found: C, 18.26; H, 1.31; N, 4.29. Calc. for $C_{10}H_8$ N_2Br_4Re (**2**): C, 18.14; H, 1.22; N, 4.23%.

2.4. Preparation of [ReBr$_3$(NO)(bipy)] (3)

NO was passing through a vigorously stirred and refluxing solution of [ReOBr$_3$(bipy)] (0.5 g, 0.84 mmol) and PPh$_3$ (1 g, 3.8 mmol) in CHBr$_3$ (60 cm^3). The reaction was carried out for 4 h. The colour changed quickly from green to dark red. Then the resulting solution was evaporated to a volume of 10 cm^3. The dark red precipitate of **3** formed by the addition of EtOH (100 cm^3) was washed with EtOH and cold ether, and dried in vacuo. Yield: 55%.

IR (KBr, cm^{-1}) 3111 (m), 3078 (m), 1737 (s), 1601 (s), 1563 (w), 1494 (m), 1467 (s), 1446 (s), 1418 (w), 1315 (m), 1235 (w), 1173 (w), 1235 (w), 1174 (w), 1122 (w), 1104 (m), 1069 (m), 1020 (m), 768 (s), 722 (m), 664 (w), 650 (m).

Anal. Found: C, 19.80; H, 1.43; N, 6.90. Calc. for $C_{10}H_8$ N_3OBr_3Re (**3**): C, 19.62; H, 1.32; N, 6.86%.

2.5. Crystal structure determination and refinement

The three-dimensional X-ray intensity data of **1** were collected on a Kuma KM-4 diffractometer, using Mo Kα radiation (graphite monochromator) in the ω–2θ scan mode, at room temperature and data of **2** were collected on a KM-4-CCD automatic diffractometer equipped with a CCD detector, with graphite monochromated Mo Kα radiation ($\lambda = 0.71073$ Å) at a temperature of 289.0(1) K, with the ω scan mode; 29 s exposure time was used and the complete Ewald sphere was collected up to $2\theta = 50.21°$. The unit cell parameters were determined from least-squares refinement of the setting angles of 3513 strongest reflections. Details concerning crystal data and refinement are given in Table 1. Examination of two reference frames monitored after each 20 frames measured for compound **2** showed 0.71% loss of the intensity. During the data reduction above the decay correction coefficient was taken into account. The Lorentz, polarization, empirical (for **1**) and numerical (for **2**) [27] absorption corrections were applied. The structure of complex **1** was solved by the Patterson method subsequently completed by difference Fourier recycling. The structure of complex **2** was solved by direct methods. All the non-hydrogen atoms in **1** and **2** were refined anisotropically using full-matrix, least-squares techniques. The hydrogen atom positions of the phenyl rings were found from subsequent difference Fourier syntheses and were refined as ‘riding’ on the adjacent carbon atom and refined with an individual isotropic temperature factor equal to 1.2 times the value of the equivalent temperature factor of the parent carbon atom. SHELXS-97 [28], SHELXL-97 [29] and SHELXTL [30] programs were used for all the calculations. Atomic scattering factors were those incorporated in the above computer programs.

Table 1
Crystal data and structure refinement for **1** and **2**

	1	**2**
Empirical formula	$C_{10}H_8N_2Br_3ORe$	$C_{10}H_8N_2Br_4Re$
Formula weight	598.11	662.02
Temperature (K)	293(2)	291(2)
Crystal system	orthorhombic	monoclinic
Space group	*Pbca*	*Pn*
Unit cell dimensions		
a (Å)	12.513(6)	8.2937(4)
b (Å)	13.431(4)	6.8536(13)
c (Å)	16.116(4)	12.7038(7)
α (°)	90	90
β (°)	90	103.277(4)
γ (°)	90	90
V (Å^3)	2708.5(17)	702.80(14)
Z	8	2
D_{calc} (Mg m^{-3})	2.934	3.128
Absolute coefficient (mm^{-1})	17.808	19.994
$F(0\,0\,0)$	2160	594
Crystal dimensions (mm)	0.08 × 0.13 × 0.34	0.17 × 0.14 × 0.14
θ Range for data collection (°)	2.53–25.10	3.90–25.10
Index ranges	$-14 \le h \le 14$ $0 \le k \le 15$ $0 \le l \le 19$	$-9 \le h \le 9$ $-8 \le k \le 8$ $-15 \le l \le 15$
Reflections collected	4626	7673
Independent reflections	2374 ($R_{int} = 0.0521$)	2452 ($R_{int} = 0.0534$)
Data/restraints/parameters	2374/0/155	2452/2/155
Goodness-of-fit on F^2	1.121	1.098
Final R indices [$I > 2\sigma(I)$]	$R_1 = 0.0461$; $wR_2 = 0.0826$	$R_1 = 0.0451$; $wR_2 = 0.1302$
R indices (all data)	$R_1 = 0.0802$; $wR_2 = 0.0949$	$R_1 = 0.0453$; $wR_2 = 0.1303$
Largest difference peak and hole (e Å^{-3})	1.727 and −0.974	2.223 and −2.093

3. Results and discussion

When gaseous nitric oxide was passed through a solution of **1** in bromoform only the starting material was recovered, but in the presence of an excess of triphenylphosphine the nitrosyl **3** was obtained. The reaction between **1** and PPh_3 in refluxing $CHBr_3$ led to the bromide rhenium(IV) complex—**2**.

Considering the facts reported previously: (i) $[ReX_4L_2]$ (X = halide and L = phosphine ligand) derivatives are usually obtained by reduction of rhenium(V) halide or oxohalide precursors or by oxidation of rhenium(III) halides and the latter process may be performed by the solvents when they are halogenated [31–33]; (ii) the $[ReCl_3(PPh_3)_2]$ complex, generated in situ from $[ReOCl_3(PPh_3)_2]$ and PPh_3, undergoes a direct reaction with the triazenido anion Li(RN–N=NR) to give the *trans*-$[ReCl_2(PPh_3)_2(RN{-}N{-}NR)]$ complex with the bidentate triazenido ligand [34]; the course of the above mentioned reactions of **1** can be easily explained. The unsaturated rhenium(III) complex $[ReBr_3(bipy)]$, generated from $[ReOBr_3(bipy)]$ and PPh_3 in the initial step, undergoes the nitrosylation reaction by NO or halogenation reaction by $CHBr_3$.

The complex **1** crystallises in the orthorhombic space group *Pbca* and its crystal structure is composed of the molecules located in general positions linked via weak intermolecular C(8)–H(8A)···O(1# $-x+1/2$, $-y$, $z-1/2$) hydrogen bonds [35–37] (D···A distance 3.24(2) Å and D–H···A angle 139.8°) to one-dimensional chain $[ReOBr_3(bipy)]$.

Table 1 presents crystal data and structure refinement for **1**, and Fig. 1 shows the numbering scheme of **1**. Three bromine ligands are in *meridional* geometry, and the coordinated bipyridine molecule, which forms a five-membered metallacycle with the metal atom is in a *trans* position towards the oxo ligand and bromine Br(2) ion. The pseudo-octahedral environment of the Re center in **1** shows clear distortions, induced mainly by the narrow bite angle of the chelating bipyridine, a multiple bonding ligand in the coordination sphere, and partially by two weak intramolecular hydrogen bonds: C(5)–H(5A)···Br(2) and C(10)–H(10A)···O(1) (D···A distance 3.465(14) and 2.85(2) Å and D–H···A angle 126.9 and 113.6°, respectively). Significant deviations from linearity are observed in O(1)–Re(1)–N(1) [161.6(4)°], Br(1)–Re(1)–Br(3) [163.42(5)°] and N(2)–Re(1)–Br(2) bond angles [168.5(3)°]. The bond angles between *cis*-ligands vary between 72.9(4)° [N(1)–Re(1)–N(2)] and 102.7(3)° [O(1)–Re(1)–Br(2)]. A similar trend is observed in other rhenium complexes containing oxo and bipyridine ligands. For example, high electronic density along the Re–O axis in *fac*-$[ReOCl_3(dppm\text{-}P,P')]$ (dppm = $Ph_2PCH_2PPh_2$) strongly influences the positions of the adjacent chlorine atoms, which are pushed away—the mean of the O–Re–Cl angles is 104°. This feature also causes a strong deviation from linearity of the O–Re–Cl(1) sequence [162.8(2)°] [38]. In $[Re(bipy)(CO)_4][PF_6]$ the *cis* bond angles are in the range from 74.6(2) to 97.3(4)°, while the *trans* bond angles vary between 171.0(2)° and 176.4(3)° [39]. The bipy bite angle in **1** [72.9(4)°] is typical for complexes containing polypyridine ligands: 70.6(3)° for *cis*-$[ReO_2(bipy)(py)_2][ClO_4]$ [35], 74.6(2)° for $[Re(bipy)(CO)_4][PF_6]$ [40] and 71.2(3)° for *cis*-$[ReO_3Cl(bipy)]$ [41]. The most important angles and bond lengths for **1** are reported in Table 2. The short Re–oxo bond length of 1.689(4) Å in **1** indicates the presence of a triple bond Re≡O [42] and is similar to the values found in other Re(V) oxo compounds: 1.669(4) Å in $[ReOCl_3(PPh_3)(OPPh_3)]$ [43] and 1.671(6) Å in *fac*-$[ReOCl_3(dppm\text{-}P,P')]$ (dppm = $Ph_2PCH_2PPh_2$) [38]. The bond valence computed as $v_{ij} = \exp[(R_{ij} - d_{ij})/0.37]$ [44–46], where R_{ij} is the bond-valence parameter (in the formal sense R_{ij} is the single-bond length between i and j atoms) [47], is $v_{Re-O} = 2.14$ v.u. (valence units), which initially suggest that Re≡O has character of double rather than triple bond. But computing the

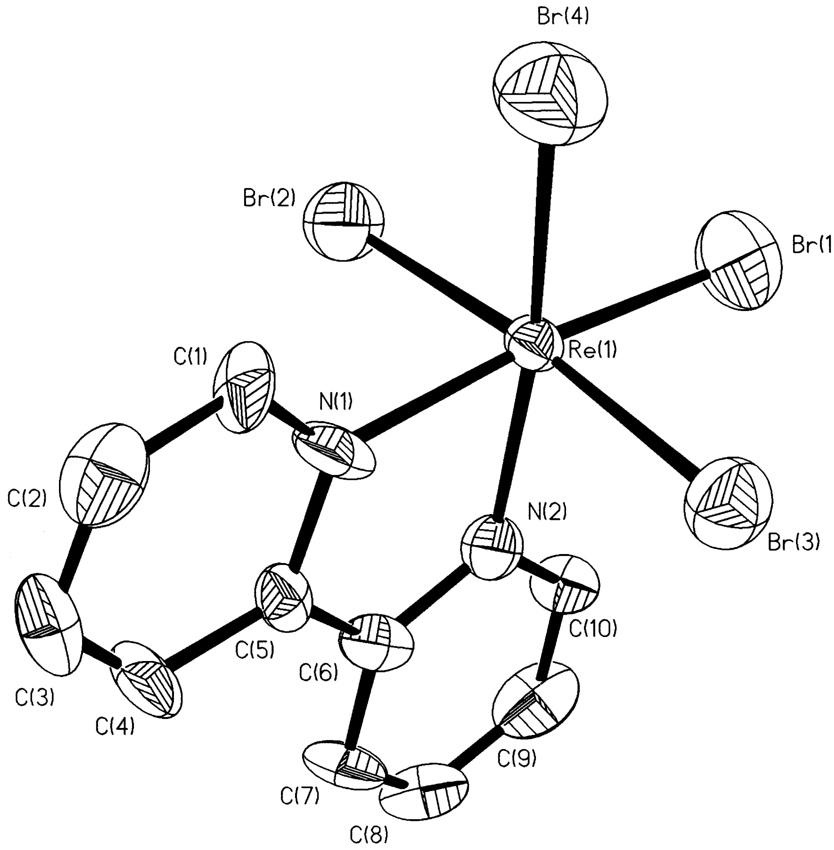

Fig. 1. The molecular structure of **1**. The thermal ellipsoids are drawn at 50% probability level.

Table 2
The selected bond lengths (Å) and angles (°) for **1**

Bond lengths		*Bond angles*	
Re(1)–O(1)	1.689(8)	O(1)–Re(1)–N(2)	88.8(4)
Re(1)–N(1)	2.257(10)	O(1)–Re(1)–N(1)	161.6(4)
Re(1)–N(2)	2.139(9)	N(2)–Re(1)–N(1)	72.9(4)
Re(1)–Br(1)	2.4896(15)	O(1)–Re(1)–Br(2)	102.7(3)
Re(1)–Br(2)	2.4639(15)	N(2)–Re(1)–Br(2)	168.5(3)
Re(1)–Br(3)	2.4912(15)	N(1)–Re(1)–Br(2)	95.6(3)
N(1)–C(1)	1.339(15)	O(1)–Re(1)–Br(1)	98.6(3)
N(1)–C(5)	1.319(15)	N(2)–Re(1)–Br(1)	89.4(3)
N(2)–C(6)	1.382(16)	N(1)–Re(1)–Br(1)	82.4(3)
N(2)–C(10)	1.313(15)	Br(2)–Re(1)–Br(1)	88.68(5)
		O(1)–Re(1)–Br(3)	97.9(3)
		N(2)–Re(1)–Br(3)	91.1(3)
		N(1)–Re(1)–Br(3)	81.9(3)
		Br(2)–Re(1)–Br(3)	87.60(5)
		Br(1)–Re(1)–Br(3)	163.42(5)
		C(1)–N(1)–C(5)	121.9(11)
		C(1)–N(1)–Re(1)	116.3(8)
		C(5)–N(1)–Re(1)	121.9(9)
		N(1)–C(1)–C(2)	120.9(12)
		N(1)–C(1)–C(6)	116.4(11)
		C(4)–C(5)–N(1)	119.9(13)
		C(6)–N(2)–C(10)	119.0(12)
		C(6)–N(2)–Re(1)	119.6(8)

remaining valences ($v_{\mathrm{Re-N}} = 0.59_{(1)}$, $0.81_{(2)}$, $v_{\mathrm{Re-Br}} = 0.90_{(1)}$, $0.96_{(2)}$, $0.89_{(3)}$ v.u, where $R_{\mathrm{Re-N}}$, $R_{\mathrm{Re-O}}$, $R_{\mathrm{Re-Br}}$ were taken as 2.06, 1.97 and 2.21 [44], respectively) gives a total Re valence $v_{\mathrm{Re}} = 6.29$ which means that the valence sum rule is violated probably by distortion of the Re environment. This can be the main reason of differences between the computed valence and the formal triple character of the Re≡O bond. The Re(1)–N(1) distance is determined by the presence of oxygen in the *trans* position. The structural *trans* effect, which is observed in complexes with short M–O bonds, results in an increase in the Re–L_{trans} distances, which is in good accordance with the computed bond valence. Table 3 shows the influence of the oxo group on the Re–N_{trans} bond distance in rhenium(V) oxo complexes.

Table 3
Selected Re–N_{trans} and Re–N_{cis} bond lengths in oxo rhenium(V) complexes

Complex	Re–N_{trans} (Å)	Re–N_{cis} (Å)	References
$[Ph_4As][ReOBr_4(NCMe)]$	2.31		[48]
trans-$[ReO_2(en)_2]Cl$		2.17 (mean)	[49]
$[Re_2O_3(en)_2Cl_4]$		2.17 (mean)	[50]
$[ReOBr_3(bipy)]$	2.257	2.139	this work

The Re–Br bond lengths in **1** (Table 2) are in good agreement with values found for [$ReBr_3(NO)(MeCN)(PPh_3)$] [2.4901(13), 2.4943(14) and 2.5294(12) Å] [15] and [$ReBr_3(NO)(OPPh_3)_2$] [2.462(3) and 2.4988(7) Å] [20].

The complex **2** belongs to the *Pn* space group and the molecular structure of **2** is shown in Fig. 2. Table 1 presents crystal data and structural refinement for **2**. The rhenium atom in **2** is in a distorted octahedral environment. Two bromine ions [Br(1), Br(4)] and two *cis*-nitrogen atoms of the bipy molecule hold the equatorial positions. The Br(2) and Br(3) ions occupy the axial positions. Similar to **1**, the narrow bipy bite angle in **2** [77.9(6)°] causes a strong departure from the ideal octahedron, the angles between *cis*-ligands vary between 77.9(6)° and 94.5(5)°, and the *trans*-angles are between 172.2(5)° and 174.19(9)°. The most important angles and bond lengths for **2** are reported in Table 4. The bond valences computed as above are: $v_{\text{Re–N}} = 0.84_{(1)}, 0.79_{(2)}$, $v_{\text{Re–Br}} = 1.09_{(1)}, 0.94_{(2)}, 0.97_{(3)}, 0.97_{(4)}$ v.u.

Although the two Re–N distances between Re and the bipy ligand are 2.124(17) and 2.145(16) Å, there is no obvious electronic cause for this difference. Thus the Re–N distances to the bipy ligand are likely to result from geometry restrains of the rigid bipyridyl group crystal packing. However, the longer Re–N bond is *trans* to the shorter Re–Br bond, which is consistent with pπ–dπ–dπ synergism involving the *trans* N–Re–

Table 4
Selected bond lengths (Å) and angles (°) for **2**

Bond lengths		*Bond angles*	
Re(1)–N(1)	2.124(17)	N(1)–Re(1)–N(2)	77.9(6)
Re(1)–N(2)	2.145(16)	N(1)–Re(1)–Br(4)	94.5(4)
Re(1)–Br(1)	2.418(3)	N(2)–Re(1)–Br(4)	172.2(5)
Re(1)–Br(2)	2.472(3)	N(1)–Re(1)–Br(1)	172.4(4)
Re(1)–Br(3)	2.458(2)	N(2)–Re(1)–Br(1)	94.5(5)
Re(1)–Br(4)	2.404(3)	Br(4)–Re(1)–Br(1)	93.10(12)
N(1)–C(1)	1.34(2)	N(1)–Re(1)–Br(3)	88.2(4)
N(1)–C(5)	1.41(2)	N(2)–Re(1)–Br(3)	88.7(4)
N(2)–C(10)	1.33(2)	Br(4)–Re(1)–Br(3)	92.58(11)
N(2)–C(6)	1.38(2)	Br(1)–Re(1)–Br(3)	91.95(10)
C(1)–C(2)	1.34(3)	N(1)–Re(1)–Br(2)	86.8(4)
C(2)–C(3)	1.35(3)	N(2)–Re(1)–Br(2)	87.3(4)
C(3)–C(4)	1.37(3)	Br(4)–Re(1)–Br(2)	90.76(11)
C(4)–C(5)	1.37(3)	Br(1)–Re(1)–Br(2)	92.60(10)
C(5)–C(6)	1.43(3)	Br(3)–Re(1)–Br(2)	174.19(9)
		C(1)–N(1)–C(5)	118.4(17)
		C(1)–N(1)–Re(1)	126.6(13)
		C(5)–N(1)–Re(1)	115.0(13)
		C(10)–N(2)–C(6)	119.6(16)
		C(10)–N(2)–Re(1)	126.8(13)
		C(6)–N(2)–Re(1)	113.6(13)
		C(2)–C(1)–N(1)	121.5(19)
		C(4)–C(5)–N(1)	118.5(17)
		N(1)–C(5)–C(6)	115.1(15)
		C(7)–C(6)–N(2)	117.1(19)
		N(2)–C(6)–C(5)	118.2(15)
		C(9)–C(10)–N(2)	122.2(19)

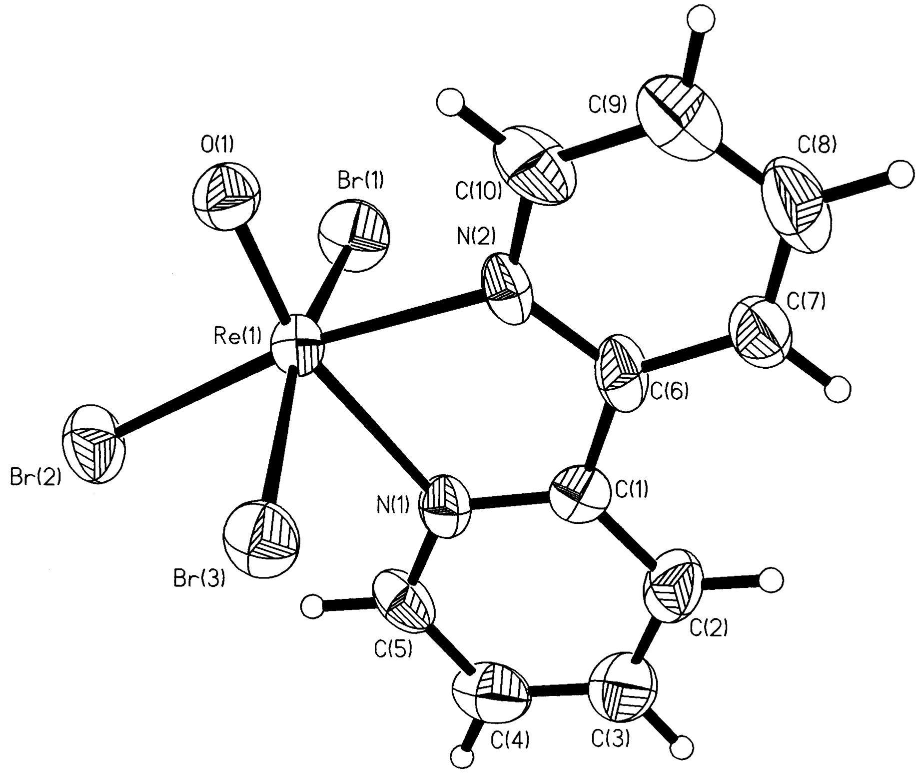

Fig. 2. The molecular structure of **2**.

Br linkage. There is also a considerable difference between the equatorial Re–Br and the axial Re–Br bonds, the former being shorter than the axial ones. A similar *trans* effect of the bipy ligand was observed in [Re(bipy)(CO)$_4$](PF$_6$) [39]. The distortion of the Re environment is also partially caused by two weak intramolecular bonds C(1)–H(1)···Br(4) and C(10)–H(10)···Br(1) (D···A distances are 3.38(2) and 3.41(2) Å and D–H···A angles are 123.9° and 124.4°, respectively). The molecules of **2** build up to a two-dimensional network via two intermolecular weak hydrogen bonds C3–H3···Br(4# $x+1/2$, $-y-1$, $z-1/2$) and C8–H8···Br(4# $x+1$, $y+1$, z); (D···A distances are 3.51(2) and 3.66(3) Å and D–H···A angles are 124.3° and 148.0°, respectively).

The IR spectrum of **1** exhibits a strong band at 982 cm^{-1} assignable to the $\nu_{\mathrm{Re=O}}$ mode. This value compares well with those reported for other rhenium(V) complexes containing a chelating ligand in the coordination sphere: [ReOBr$_3$(dppen)] (dppen = *cis*-Ph$_2$PCH=CHPPh$_2$)—984 cm^{-1}, [ReOBr$_3$(dppm)] (dppm = Ph$_2$PCH$_2$PPh$_2$)—980 cm^{-1} and [ReOBr$_3$(dppe)] (dppe = Ph$_2$PCH$_2$CH$_2$PPh$_2$)—982 cm^{-1} [51]. A strong band at 1737 cm^{-1}, corresponding to ν_{NO} in the spectrum of **3**, confirms the presence of a nitrosyl group. This is consistent with the linear NO range of Haymore and Ibers (ν_{NO} above 1620–1610 cm^{-1} that were assigned to linear M–N–O systems, while ν_{NO} below 1610 cm^{-1} were assigned to bent M–N–O systems) [52]. Most nitrosyl rhenium(I) complexes of the type [ReX$_3$(NO)L$_2$], where L is a monodentate arsine, oxygen or phosphorus donor ligand, show a ν_{NO} very close to 1735 cm^{-1}, for example: [ReCl$_3$(NO)(PPh$_3$)] 1734 cm^{-1} [18], [ReBr$_3$(NO)(OPPh$_3$)$_2$] 1738 cm^{-1} [20] and [ReCl$_3$(NO)(AsPh$_3$)$_2$][ReCl$_4$(AsPh$_3$)$_2$] 1733 cm^{-1} [21]. The other bands in the IR spectra of **1**–**3** confirm the presence of the bipy ligand in the coordination sphere.

Complex **1** is diamagnetic, and compounds **2** and **3** are paramagnetic with an effective magnetic moment 3.48 and 1.73 BM, respectively. These values of effective magnetic moment indicate the presence of three and one unpaired electrons in **2** and **3**, respectively.

The positions and molar absorption coefficients of electronic bands for complexes **1**–**3** and the electronic transitions assigned to the bands are shown in Table 5.

The absorption bands shown in Table 5 indicate the pseudo-octahedral symmetry of complexes **1**–**3**. The highest decrease in symmetry of complex **1** allows the observation intercombination transitions. The assignments of the absorption bands remain in full accordance with X-ray data. The shorter Re–N(2) bond [2.139(9) Å] and longer N(2)–C bond [average 1.3475 Å] for complex **1** in comparison with Re–N(1) [2.257(10) Å] and shorter N(1)–C [average 1.329 Å], testify the fact that the band at 32 570 cm^{-1} corresponds with $5d_{xy} \rightarrow \pi^*$ charge transfer onto the bipy ring in the *trans* position towards Br(2), with simultaneous donor action pπ–dπ Br(2), proved by the length of Re–Br(2) bond being shorter than Re–Br(1) and Re–Br(3) distances. In complex **2** the bond lengths of Re–N [2.124(17) and 2.145(16) Å], N(1)–C and N(1)–C [1.375 and 1.355 Å, respectively] prove the charge transfer onto both bipy rings. Analogically, Re–Br bond lengths in *trans* positions towards bipy nitrogen atoms are in complex **2** shorter than the other Re–Br bond lengths. However, weak donor ability of Br$^-$ ions and weak acceptor ability of bipy only slightly increase the degree of covalency of the coordination bond, which is also shown by elongation of the N–C bond (ca. 0.02 Å) in comparison with a free molecule of bipy [53]. Therefore, the significantly higher value of the 10 Dq parameter both in complex **1** and in complex **2** is caused by the presence of the oxo ligand and higher oxidation state of the central atom. That is why the Racah B parameter in complex **2** is significantly higher than in complex **1**, and $\beta_{55} = 0.9$ proves the dominant role of the ion bond in complex **2**, causing stabilization of a high spin state $(b_2)^1(e)^2$. A low spin state $(b_2)^2$ is stabilized in complex **2**. The influence of

Table 5
Band positions, molar absorption coefficients and assignments for **1**–**3** complexes

[ReOBr$_3$(bipy)] (**1**)			[ReBr$_4$(bipy)] (**2**)			[ReBr$_3$(NO)(bipy)] (**3**)		
Band position (cm^{-1})	ε	Assignment	Band position (cm^{-1})	ε	Assignment	Band position (cm^{-1})	ε	Assignment
12 950	45	$^1A_1 \rightarrow {}^3T_2$	26 200	1680	$^4A_2 \rightarrow {}^4T_2$	24 690	1340	$^2T_2 \rightarrow {}^2A_2$
18 020	30	$^1A_1 \rightarrow {}^3T_1$	28 750	2670	$^4A_2 \rightarrow {}^4T_1(F)$ $e \rightarrow \pi^*_{\mathrm{bipy}}$	26 330	1790	$^2T_2 \rightarrow {}^2E$ $e \rightarrow \pi^*_{\mathrm{NO}}$
21 740	1250	$^1A_1 \rightarrow {}^1T_2$	33 250	4290	$^4A_2 \rightarrow {}^4T_1(P)$ $b_2 \rightarrow \pi^*_{\mathrm{bipy}}$	28 800	3140	$e \rightarrow \pi^*_{\mathrm{bipy}}$
23 310	1240	$^1A_1 \rightarrow {}^1T_1$	39 840	6720	$\pi \rightarrow \pi^*_{\mathrm{bipy}}$	31 570	7070	$^2T_2 \rightarrow {}^2A_1$ $b_2 \rightarrow \pi^*_{\mathrm{bipy}}$
32 570	8000	$b_2 \rightarrow \pi^*_{\mathrm{bipy}}$				32 720	8780	$b_2 \rightarrow \pi^*_{\mathrm{bipy}}$
42 730	7880	$\pi \rightarrow \pi^*_{\mathrm{bipy}}$ $\pi \rightarrow \pi^*_{\mathrm{Re=O}}$				40 680	9550	$\pi \rightarrow \pi^*_{\mathrm{bipy}}$

ε, molar absorption coefficient (dm^3 mol^{-1} cm^{-1}).

Table 6
The values of 10 Dq and *B* parameters for **1**–**3** complexes

Complex	10 Dq (cm^{-1})	*B* (cm^{-1})
[$ReOBr_3$(bipy)] (**1**)	27 510	480
[$ReBr_4$(bipy)] (**2**)	26 200	588
[$ReBr_3$(NO)(bipy)] (**3**)	26 330	437

trans O(1) on bipy is opposite in comparison with the bromide ions influence. The multiplicity of the Re=O bond, smaller O^{2-} ion radius and r_{Re}, and higher electronegativity of oxygen cause the shift of electron density onto O^{2-}, making $5d \rightarrow \pi^*$ charge transfer onto bipy ring in the *trans* position towards O(1) impossible. In complexes **2** and **3** two charge transfer bands $5d \rightarrow \pi^*_{bipy}$ are observed; the higher frequency bands are more intense (as $5d \rightarrow \pi^*_{NO}$ transitions in complex **3**) because of the symmetry. Both the presence of the NO group in complex **3**, and stronger donor ability of Re(II) increases the degree of covalency of complex **3** (the lowest Racah *B* parameter). That is why the pairing energy ($p = 12\,020$ cm^{-1}) is significantly lower than 10 Dq, causing stabilization of the low spin state $(b_2)^2(e)^3$. The values of 10 Dq and *B* parameters for **1**–**3** complexes are presented in Table 6. Diamagnetism of complex **1** and magnetic moments of complexes **2** and **3** confirm the spectroscopic data.

4. Supplementary data

Supplementary data are available from the CCDC, 12 Union Road, Cambridge CB2 1EZ, UK on request, quoting the depositions numbers: 200393 ([$ReOBr_3$(bipy)]), 200394 ([$ReBr_4$(bipy)]) (fax: +44-1223-336033; e-mail: deposit@ccdc.cam.ac.uk or www: http://www.ccdc.cam.ac.uk).

Acknowledgements

The crystallographic part of compound **2** was financed by funds allocated by the State Committee for Scientific Research to the Institute of General and Ecological Chemistry, Technical University of Łódz.

References

[1] K.G. Caulton, Coord. Chem. Rev. 14 (1975) 317.
[2] B. Hussain-Bates, M.B. Hursthouse, Polyhedron 9 (1990) 2081.
[3] B.S. McGilligan, J. Arnold, G. Wilkinson, B. Hussain-Bates, M.B. Hursthouse, J. Chem. Soc., Dalton Trans. (1990) 2465.
[4] C.M.T. Hayward, J.P. Folkers, J.R. Shapley, Inorg. Chem. 27 (1988) 3685.
[5] R. Bhattacharyya, J. Chem. Soc., Dalton Trans. (1988) 794.
[6] G.B. Richter-Addo, P. Legzdins, Metal Nitrosyls, Oxford University Press, Oxford, 1992.
[7] M. Leconte, Y.B. Taarit, J.L. Bilhou, J.M. Basset, J. Mol. Catal. 8 (1980) 263.
[8] R.M.J. Palmer, A.G. Ferrige, S. Moncada, Nature 327 (1987) 524.
[9] S. Moncada, R.M.J. Palmer, E.A. Higgs, Pharmacol. Rev. 43 (1991) 109.
[10] P.L. Feldman, O.W. Griffith, D.J. Stuehr, Chem. Eng. News 71 (1993) 26.
[11] J.O. Dziegielewski, K. Filipek, B. Machura, Polyhedron 14 (1995) 555.
[12] J.O. Dzięgielewski, B. Machura, T. Kupka, in: J.C. Merlin, S. Turrell, J.P. Huvenne (Eds.), Spectroscopy of Biological Molecules, Kluwer Academic Publishers, Dortrecht, 1995, p. 589.
[13] J.O. Dzięgielewski, B. Machura, J. Marek, Polyhedron 15 (1996) 3713.
[14] J.O. Dzięgielewski, B. Machura, T.J. Bartczak, Polyhedron 15 (1996) 2813.
[15] T.J. Bartczak, W. Czurak, J.O. Dzięgielewski, B. Machura, Polish J. Chem. 72 (1998) 633.
[16] J.O. Dzięgielewski, B. Machura, T. Kupka, T.J. Bartczak, W. Czurak, Polish J. Chem. 72 (1998) 1009.
[17] J.O. Dzięgielewski, B. Machura, T.J. Bartczak, W. Czurak, J. Kusz, J. Warczewski, J. Coord. Chem. 48 (1999) 125.
[18] T.J. Bartczak, W. Czurak, J.O. Dzięgielewski, B. Machura, A. Jankowska, J. Kusz, J. Warczewski, Polyhedron 18 (1999) 2313.
[19] T.J. Bartczak, W. Czurak, J.O. Dzięgielewski, B. Machura, J. Kusz, J. Warczewski, Polish J. Chem. 74 (2000) 265.
[20] T.J. Bartczak, W. Czurak, J.O. Dzięgielewski, B. Machura, A. Jankowska, J. Kusz, J. Warczewski, J. Coord. Chem. 52 (2001) 361.
[21] B. Machura, J.O. Dzięgielewski, S. Michalik, T.J. Bartczak, R. Kruszynski, J. Kusz, Polyhedron 21 (2002) 2167.
[22] Y. Wang, J.J.R. da Silva Fraústo, A.J.L. Pombeiro, J. Organomet. Chem. 476 (1994) C9.
[23] Y. Wang, J.J.R. da Silva Fraústo, A.J.L. Pombeiro, M.A. Pellinghelli, A. Tiripicchio, J. Organomet. Chem. 430 (1992) C56.
[24] I. Ara, R.A. Walton, Inorg. Chim. Acta 198–200 (1992) 787.
[25] M.C. Chakravorti, J. Indian Chem. Soc. 44 (1967) 809.
[26] G. Rouschias, Chem. Rev. 74 (1974) 531.
[27] X-RED. Version 1.18. STOE and Cie GmbH, Darmstadt, Germany (1999).
[28] G.M. Sheldrick, Acta Crystallogr., Sect. A 46 (1990) 467.
[29] G.M. Sheldrick, SHELXL-97. Program for the Refinement of Crystal Structures, University of Göttingen, Germany, 1997.
[30] G.M. Sheldrick, SHELXTL: Release 4.1 for Siemens Crystallographic Research Systems (1990).
[31] J. Chatt, J.D. Garforth, N.P. Johnson, G.A. Rowe, J. Chem. Soc. (1967) 601.
[32] G. Rouschias, G. Wilkinson, J. Chem. Soc. A (1966) 465.
[33] G. Rouschias, G. Wilkinson, J. Chem. Soc. A (1967) 993.
[34] R. Rossi, A. Duatti, L. Magon, U. Casellato, R. Graziani, L. Tonialo, J. Chem. Soc., Dalton Trans. (1982) 1949.
[35] G.R. Desiraju, T. Steiner, The Weak Hydrogen Bond in Structural Chemistry and Biology, Oxford University Press, Oxford, 1999.
[36] G.A. Jeffrey, W. Saenger, Hydrogen Bonding in Biological Structures, Springer, Berlin, 1994.
[37] R. Taylor, O. Kennard, J. Am. Chem. Soc. 104 (1982) 5063.
[38] R. Rossi, A. Marchi, L. Marvelli, L. Magon, M. Peruzzini, U. Casellato, R. Graziani, Inorg. Chim. Acta 204 (1993) 63.
[39] G.F. Strouse, H.U. Güdel, V. Bertolasi, V. Ferretti, Inorg. Chem. 34 (1995) 5578.
[40] R.L. Blackbourn, L.M. Jones, M. Sabat, J.T. Hupp, Inorg. Chem. 29 (1990) 1791.
[41] W.S. Sergiyenko, T.S. Khodashova, M.A. Porai-Koshits, L.A. Butman, Koord. Khim. 3 (1977) 1060.

[42] J.M. Mayer, Inorg. Chem. 27 (1988) 3899.
[43] J.C. Bryan, M.C. Perry, J.B. Arterburn, Acta Crystallogr., Sect. C 54 (1998) 1607.
[44] I.D. Brown, Acta Crystallogr., Sect. B 48 (1992) 553.
[45] I.D. Brown, Acta Crystallogr., Sect. B 53 (1997) 381.
[46] M. O'Keeffe, N.E. Brese, J. Am. Chem. Soc. 113 (1991) 3226.
[47] L. Sieron, M. Bukowska-Strzyzewska, Acta Crystallogr., Sect. C 55 (1999) 1230.
[48] F.A. Cotton, S.J. Lippard, Inorg. Chem. 5 (1966) 416.
[49] W.S. Sergiyenko, M.A. Porai-Koshits, T.S. Khodashova, J. Strukt. Chimi 15 (1974) 275.
[50] T. Głowiak, T. Lis, B. Jezowska-Trzebiatowska, Bull. Acad. Polon. Sci. Ser. Sci. Chim. 20 (1972) 199.
[51] X.L.R. Fontaine, E.H. Fowles, T.P. Layzell, B.L. Shaw, M. Thornton-Pett, J. Chem. Soc., Dalton Trans. (1991) 1519.
[52] B.L. Haymore, I.A. Ibers, Inorg. Chem. 14 (1975) 3060.
[53] M.H. Chisholm, J.C. Huffman, I.P. Rothwell, P.G. Bradley, N. Kress, W.H. Woodruff, J. Am. Chem. Soc. 103 (1981) 4945.